Cellular normoxic biophysical markers of hydroxyurea treatment in sickle cell disease

Poorya Hosseini[a,b,c], Sabia Z. Abidi[d], E Du[e], Dimitrios P. Papageorgiou[d], Youngwoon Choi[f], YongKeun Park[g], John M. Higgins[h], Gregory J. Kato[i], Subra Suresh[j,k,l,1], Ming Dao[d,1], Zahid Yaqoob[a,1], and Peter T. C. So[a,b,c]

[a]Laser Biomedical Research Center, Massachusetts Institute of Technology, Cambridge, MA 02139; [b]Department of Mechanical Engineering, Massachusetts Institute of Technology, Cambridge, MA 02139; [c]Department of Biological Engineering, Massachusetts Institute of Technology, Cambridge, MA 02139; [d]Department of Materials Science and Engineering, Massachusetts Institute of Technology, Cambridge, MA 02139; [e]Department of Ocean and Mechanical Engineering, Florida Atlantic University, Boca Raton, FL 33431; [f]School of Biomedical Engineering, Korea University, Seoul 136-701, Korea; [g]Department of Physics, Korea Advanced Institute of Science and Technology, Daejeon 34141, Republic of Korea; [h]Department of Systems Biology, Harvard Medical School, Boston, MA 02115; [i]Department of Medicine, Division of Hematology–Oncology, University of Pittsburgh, Pittsburgh, PA 15261; [j]Department of Biomedical Engineering, Carnegie Mellon University, Pittsburgh, PA 15213; [k]Department of Materials Science and Engineering, Carnegie Mellon University, Pittsburgh, PA 15213; and [l]Department of Computational Biology, Carnegie Mellon University, Pittsburgh, PA 15213

Contributed by Subra Suresh, June 29, 2016 (sent for review May 21, 2016; reviewed by Joseph DeSimone and Guruswami Ravichandran)

Hydroxyurea (HU) has been used clinically to reduce the frequency of painful crisis and the need for blood transfusion in sickle cell disease (SCD) patients. However, the mechanisms underlying such beneficial effects of HU treatment are still not fully understood. Studies have indicated a weak correlation between clinical outcome and molecular markers, and the scientific quest to develop companion biophysical markers have mostly targeted studies of blood properties under hypoxia. Using a common-path interferometric technique, we measure biomechanical and morphological properties of individual red blood cells in SCD patients as a function of cell density, and investigate the correlation of these biophysical properties with drug intake as well as other clinically measured parameters. Our results show that patient-specific HU effects on the cellular biophysical properties are detectable at normoxia, and that these properties are strongly correlated with the clinically measured mean cellular volume rather than fetal hemoglobin level.

sickle cell anemia | biomarkers | cell volume | cell deformability | cellular properties

Sickle cell disease (SCD), an autosomal recessive disease, resulted in 176,000 deaths worldwide in 2013 (1). In SCD, a point mutation occurs in the gene responsible for the production of β-chain in hemoglobin (Hb), the main protein in red blood cells (RBCs) that is responsible for oxygen transport (2). This mutation changes the hydrophilic glutamic acid to a hydrophobic valine amino acid residue in the β-globin chain gene, giving rise to hemoglobin S (HbS), a variant form of Hb. Under low-oxygen (hypoxic) conditions, the hydrophobic residues within cytosol associate with one another to form polymerized fibers that alter the RBC shape (3). Although these fibers "melt" when cells experience normal oxygen (normoxic) environments, irreversible damage results from repeated exposure to alternating low-oxygen and normoxic environments, thereby giving rise to stiffer sickle RBCs (sRBCs). These sRBCs adversely affect blood flow and are associated with vessel occlusion, poor oxygen transport, and hemolysis (4). The ensuing painful episodes of vasoocclusive crises can additionally cause tissue injury that is another pathological effect associated with the disease (3, 5).

Despite the wealth of information known about SCD, optimal treatments do not exist. Patients suffering from SCD can ameliorate their disease severity with blood transfusions, and through treatment involving hydroxyurea (HU), which is the only drug for SCD approved by US Food and Drug Administration (FDA), or by recourse to pain management drugs such as opiates. Studies have shown that intake of HU, among other effects, increases the fraction of fetal Hb (HbF) in the RBCs (6). The corresponding reduction in the concentration of HbS delays polymerization of HbS upon deoxygenation, thereby reducing the probability of sickling and minimizing the resultant deleterious consequences (7). There have been other therapeutic agents that have been shown to increase production of HbF as well; however, none of them is currently approved by the FDA (8, 9). Other effects of HU administration in SCD patients on RBCs include larger cell volumes (10), increased antioxidant activity (11), reduced adhesiveness (12–14), and greater filterability (15). Mechanisms underlying these and other beneficial effects of the drug affecting leukocytes and the endothelium (16–18) have not been fully elucidated. Nevertheless, the consensus for management of SCD care is administration of HU due to its success in both adult and children populations (19–23). It must be noted, however, that there are patient populations who are unresponsive to HU treatment (24). Identifying patient-specific markers that predict HU effectiveness would, therefore, greatly improve SCD care.

Clinical studies have demonstrated that there exists a high degree of diversity in response to HU treatment among those homozygous for HbS even among identical molecular signatures (25). Multiple studies have indicated either a lack of, or weak, correlation between clinical outcome and molecular markers such as volume fraction of the HbS in the blood (25–28). Although biochemical markers alone cannot fully describe disease severity or effectiveness of treatment, biophysical markers may provide a complementary pathway to gaining insight into disease

Significance

There exists a critical need for developing biomarkers reflecting clinical outcomes and for evaluating the effectiveness of treatments for sickle cell disease patients. Prior attempts to find such patient-specific markers have mostly relied upon chemical biomarkers or biophysical properties at hypoxia with limited success. We introduce unique biomarkers based on characterization of cellular biophysical properties at normoxia and show that these markers correlate sensitively with treatment using hydroxyurea (HU), the only US Food and Drug Administration (FDA)-approved drug for sickle cell disease patients. Our unique choice of cellular biophysical markers strongly correlates with mean cellular volume rather than fetal hemoglobin level, which provides insights into possible mechanisms through which HU treatment results in beneficial clinical outcomes.

Author contributions: P.H., S.Z.A., Y.P., J.M.H., G.J.K., S.S., M.D., Z.Y., and P.T.C.S. designed research; P.H., S.Z.A., E.D., D.P.P., and Y.C. performed research; P.H., S.Z.A., E.D., D.P.P., Y.C., Y.P., J.M.H., G.J.K., S.S., M.D., Z.Y., and P.T.C.S. analyzed data; and P.H., S.Z.A., G.J.K., S.S., M.D., Z.Y., and P.T.C.S. wrote the paper.

Reviewers: J.D., University of North Carolina, Chapel Hill; and G.R., California Institute of Technology.

The authors declare no conflict of interest.

Freely available online through the PNAS open access option.

[1]To whom correspondence may be addressed. Email: mingdao@mit.edu, zyaqoob@mit.edu, or suresh@cmu.edu.

This article contains supporting information online at www.pnas.org/lookup/suppl/doi:10.1073/pnas.1610435113/-/DCSupplemental.

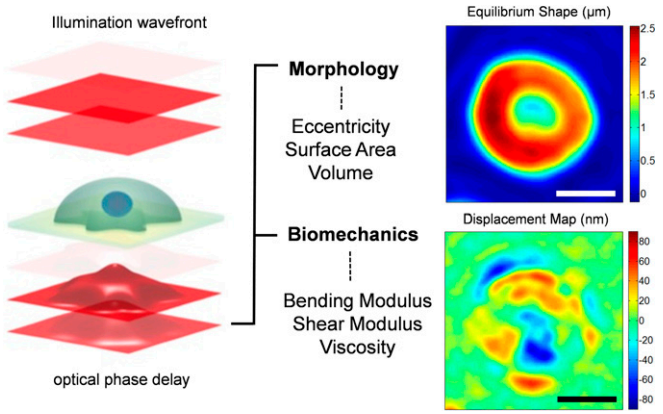

Fig. 1. Optical measurement of morphological properties of RBCs. Morphological information about the sample (eccentricity, surface area, and volume) can be obtained from deformations of the optical wave front after its traversal through RBCs. The phase delay of the optical wave front after passing through the sample is related to optical properties and morphology of the sample, and can be accurately measured through advanced interferometry. Accurate measurements of the morphology over time reveal thermal fluctuations that cause out-of-plane displacements of the cell membrane (bottom right image), which provide insights into the biomechanical properties of the whole cell (bending and shear modulus as well the cytosol viscosity). (Scale bars: 4 μm.)

pathophysiology (29). As the primary consequence of mutation in the β-globin chain gene is formation of HbS fibers within the cytosol under low-oxygen environment, biophysical studies have been mainly focused on identifying biomarkers under hypoxic condition. Measuring rheological properties of the blood under hypoxia has been suggested as one such indicator of the propensity for vaso-occlusive crisis in sickle patients (29, 30). Here, we hypothesize that biophysical properties of individual RBCs of sickle patients at normoxia, including morphology and biomechanical properties, could better characterize physiological changes due to HU treatment than molecular-level markers. Our hypothesis is based on the assumption that normoxic biophysical properties of red cells are affected by what they have undergone while circulating in blood of the patients such as repeated cycles of blood oxygenation and deoxygenation. We measure these biophysical properties using a common-path interferometric technique comparing patients who are on and off HU treatment. Comparison between the biophysical properties of RBCs and clinically measured parameters for SCD patients indicates that biomechanical properties and morphology at the individual-cell level can provide insights into the effectiveness of HU treatment, possibly leading to a better understanding of the mechanism underlying the drug.

Results

Density-Dependent Biophysical Properties of Individual Red Cells. Common-path interferometric microscopy enables noninvasive and quantitative measurements of the morphological features of the biological samples at the nanometer scale (31). These microscopes have previously been used to study morphological and biomechanical properties of the RBCs (32, 33). Fig. 1 shows the range of biophysical properties that can be assessed by measuring the morphology of RBCs and monitoring this morphology over time at the millisecond timescale. However, such measurements in transmission-type interferometers are affected by the refractive index (RI) differences of individual cells, and an average value is typically assumed for the entire cell population under investigation. The RI of RBCs is directly related to the concentration of proteins in cytosol, which, in the case of RBCs, is composed mainly of Hb. Accounting for such variations is vital in the case of RBCs of SCD patients, in particular, because they exhibit wider distributions of Hb concentrations (34, 35) than healthy patients. In this study, the accuracy of the biophysical measurements has been enhanced by subdividing blood samples from SCD patients into four densities and quantifying density-dependent properties of individual RBCs. This density separation additionally allows for decoupling Hb concentration from other biophysical properties for individual RBCs. RBCs with shapes that deviate the most from the normal biconcave shape tend to occur in the denser populations (Fig. 2), populations that are generally absent in healthy human blood. It has been suggested that these cells have been irreversibly damaged either through the normal aging process or from repeated cycles of oxygenation and deoxygenation during blood circulation (36). In general, within the first two fractions, most cells were discocytes, whereas fraction III included discocytes and some elliptical and irreversibly sickled cells. The highest number of elliptical and irreversibly sickled cells was observed in fraction IV with fewer discocytes present (Fig. 2).

Fig. 3 shows cell membrane fluctuations as a function of cell density. The average amplitude of membrane fluctuations or "flickering" is inversely proportional to the overall stiffness of the cell, that is, softer cells show larger fluctuations. This trend is consistent with previous findings on membrane fluctuations of different types of RBCs (37). The overall stiffness of the cells increases with an increase in the Hb concentration within the cytosol. The increase in cell membrane stiffness can be extracted from fluctuation amplitude data by recourse to theoretical analysis (32, 38). Specifically, this analytical model links membrane fluctuations to four biomechanical properties: in-plane shear modulus (μ), bending stiffness (κ), and area expansion modulus (K_A) of the cell membrane, as well as the viscosity of the cytosol (η). Within the range of RBC Hb concentrations in sickle cell patients, microviscosity of the Hb solution can be linked to the concentration of the Hb (39). Fractionation of the RBCs into four density categories before the measurements enables us to estimate the average viscosity value in each density fraction. Additionally, the area expansion modulus of the cell membrane,

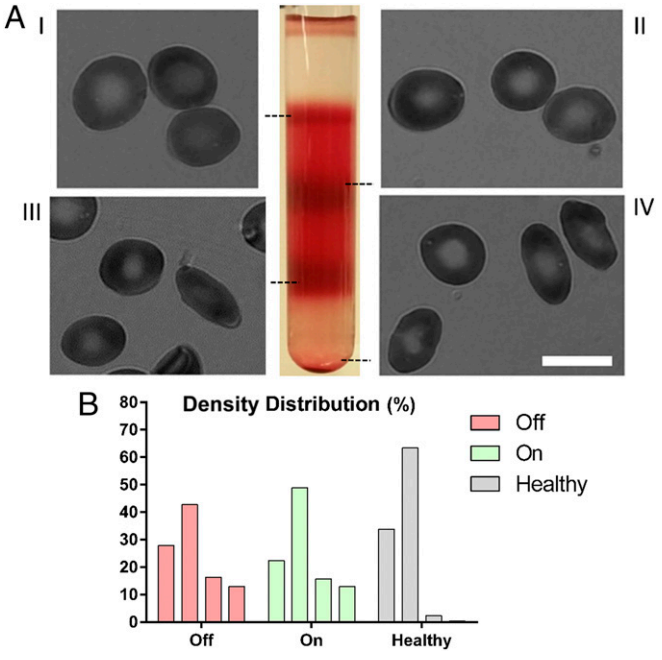

Fig. 2. Density fractionation of RBCs from sickle patients and healthy donors. (*A*) Representative images of RBCs in each density fraction from blood sample of a sickle patient. I, II, III, and IV represent density fractions that are 26.6, 30.2, 34.1, and 37.8 g·dL^{-1}, respectively. (*B*) Representative distribution of density volume percentage in sickle cell patients both on and off drug as well as healthy donors. RBCs of sickle patients, regardless of HU treatment, have denser fractions (III and IV) that are absent from healthy blood. (Scale bar: 10 μm.)

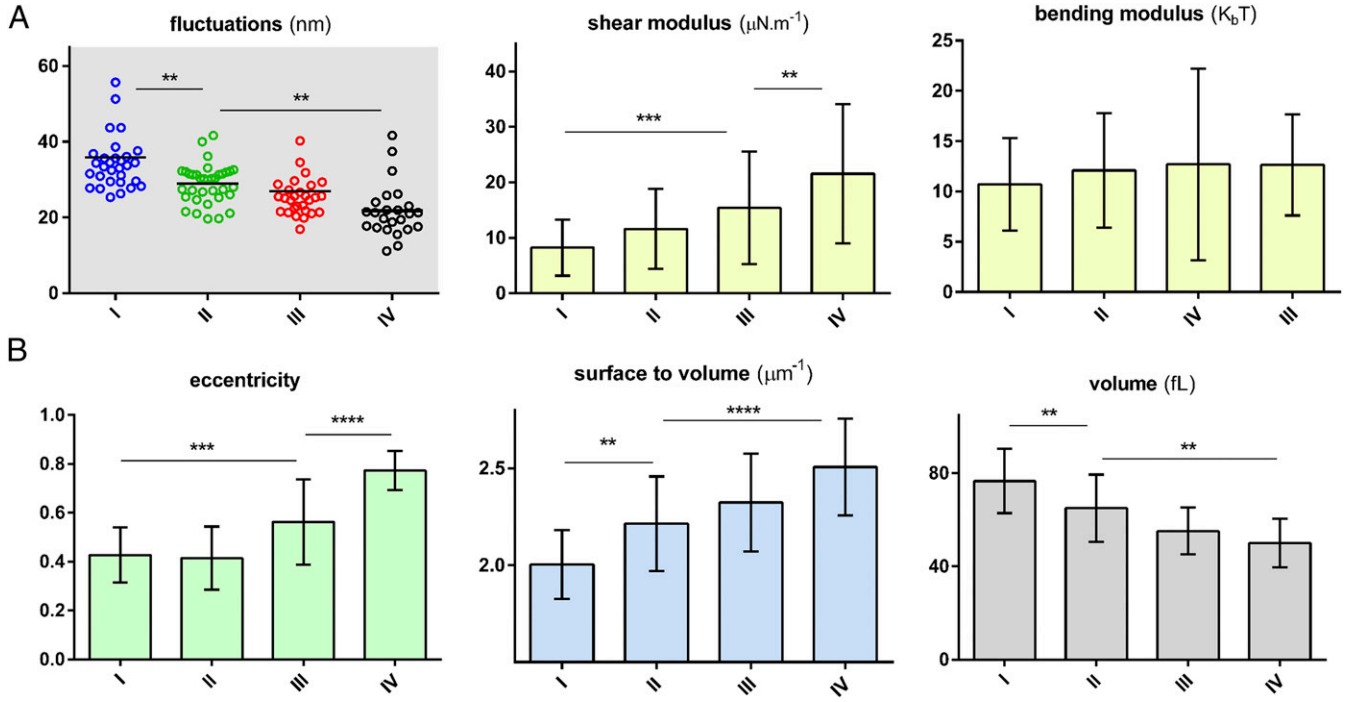

Fig. 3. Biophysical response of the RBCs of sickle patients as a function of cell density. (*A*) Biomechanical properties of the RBCs as a function of cell density. Each data point represents an individual RBC within the indicated fraction. The black horizontal line represents the mean value within the cell distribution. (*B*) By measuring the 3D shape of RBCs, morphological properties of relevance have been plotted as a function of the cell density. To calculate eccentricity, initially an ellipse is fitted to each RBC and minor axis (*b*) and major axis (*a*) of the ellipse are measured. The eccentricity ratio is then calculated as $\{1 - (a/b)^2\}^{1/2}$. The bar graphs denote mean values, whereas error bars represent ±SD. The plotted data correspond to patient III as identified in Table S1. Standard two-tailed *t* tests were used to determine the significance of the difference between two groups of data, where $^{**}P < 0.01$, $^{***}P < 0.001$, and $^{****}P < 0.0001$.

dominated by the properties of the lipid bilayer, has been well characterized using micropipette measurements (40). Therefore, viscosity of the cytosol and area expansion modulus of the cell membrane corresponding to literature values are held constant in our model for each density fraction. Thereafter, shear and bending moduli have been extracted from a fit of the experimental membrane fluctuations to the analytical model.

As seen in Fig. 3, there is a steady increase in the shear modulus of the cell membrane as the cell density increases, whereas bending modulus remains relatively constant for all density fractions. It has been suggested (32, 38) that changes in shear modulus can be attributed to the spectrin network supporting the cell membrane, whereas bending properties are mainly a function of the configuration of phospholipids, fatty acids, and cholesterols in the RBC membrane. These results are consistent with previous reports that the mechanical damage of RBCs is mainly caused by the rearrangement of the membrane scaffold proteins rather than a change in lipid bilayer or integral proteins (41, 42).

The topographic information obtained using this technique could offer insights into our understanding of SCD pathophysiology. Cellular volume and the ratio of surface area to volume of the RBCs are two such important geometric markers. The surface area-to-volume ratio in particular along with cytoplasmic viscosity and membrane stiffness regulate deformability of red cells necessary for oxygen delivery to tissues and organs (43, 44). They also affect the deformability of RBCs, which becomes critical when they pass through narrow capillaries. As seen in Fig. 3, average cell volume decreases as cell density increases. This decrease in volume is accompanied by an increase in the surface area-to-volume ratio. An additional geometric factor of potential relevance to the pathophysiology of the RBCs is the eccentricity of the individual cells. Formation of the polymerized HbS in the cytosol results in forces on the cell membrane that could occur repeatedly as cells experience cycles of oxygenation and deoxygenation. As seen in Fig. 3, the eccentricity of the denser cells is significantly higher than that of lower density cells. However, among less dense cells, there is no statistically significant difference in eccentricity. This suggests that denser RBCs in blood experience some irreversible changes in shape that are associated with changes in the skeletal or membrane proteins that regulate the biconcave shape of normal RBCs.

Effects of HU Treatment on Cellular Biomarkers. To assess the effect of HU on the biomechanical and morphological properties, we examined RBCs from patients "on" and "off" HU treatment. All measurements from such on-drug and off-drug populations were grouped together for each density category, as shown in Fig. 4, to illustrate the overall effect of drug treatment. For almost all properties and all density categories, a statistically significant difference was observed as a result of HU treatment. Bending modulus of the cell membrane has been excluded from this comparison because a specific trend was not observed for individual patients as shown in Fig. 3.

These results show that RBCs under HU treatment are softer on average regardless of their density. Shear modulus extracted from membrane fluctuations using the analytical model shows a corresponding decrease in the membrane rigidity for the on-drug population. RBCs of patients under HU treatment exhibit a higher volume and a smaller ratio of surface area to volume, on average. There was no clear difference between average eccentricity value for lighter sickle cells; however, denser cells did exhibit a higher eccentricity ratio for patients off HU treatment.

Correlation of Biophysical Properties with Clinical Measurements. There is a range of clinically measured parameters that provide insights into the pathways and effectiveness of HU therapy for SCD patients. These laboratory parameters are broadly derived from either cellular evaluation tests such as hematocrit and mean corpuscular volume (MCV), or from the molecular profile tests such as those involving blood composition using gel

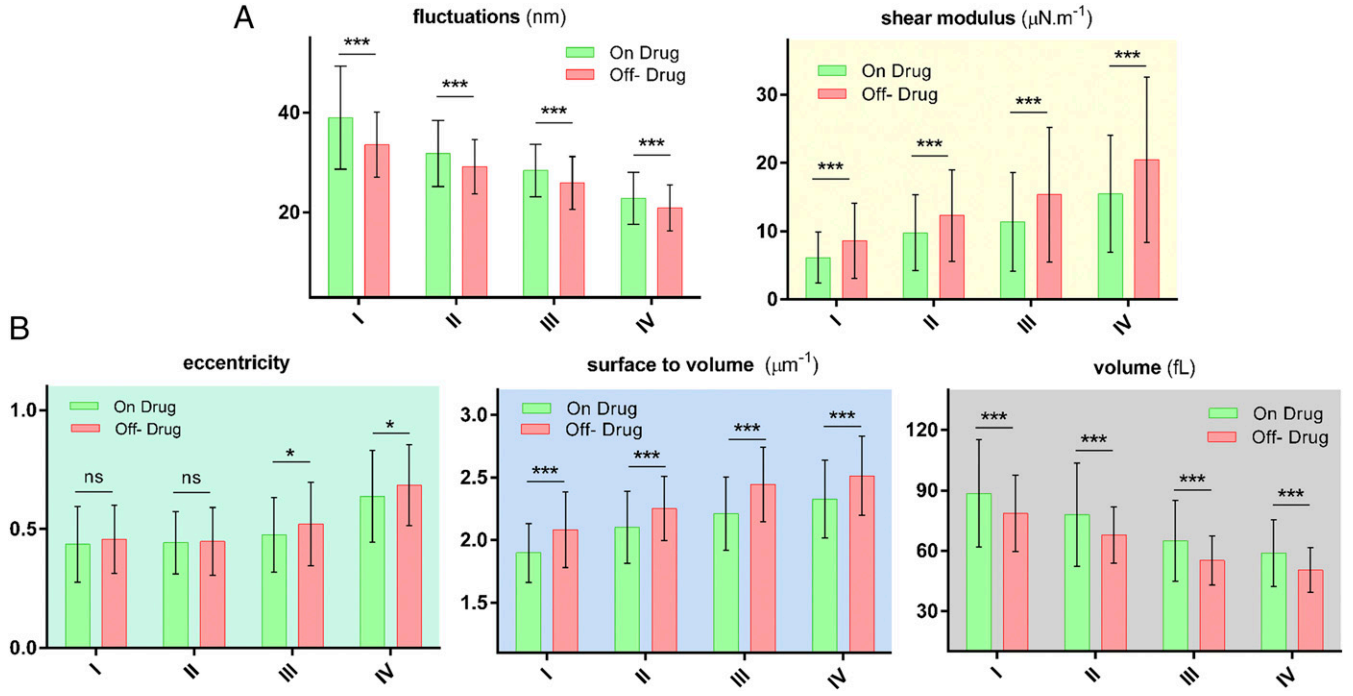

Fig. 4. Biophysical properties of individual RBCs for "on" and "off" HU drug patients. (*A*) Biomechanical properties as a function of four different cell densities. (*B*) Morphological parameters as a function of cell density. The number of measurements per patient for each density categories varies between 20 and 25 incidents. The exact numbers for each measurement are as follows: N_{on} = 126, 136, 136, and 128, and N_{off} = 172, 187, 164, and 165, for density I, II, III, and IV, respectively. The height of bar graph in each case represents the mean value, whereas the vertical error bars represent ±SD. Standard two-tailed *t* tests were used to determine the significance of the difference between two groups of data, where $*P < 0.05$, $***P < 0.001$, and "ns" indicates $P > 0.05$.

electrophoresis. These parameters are listed in *Supporting Information* for all patients in this study. Two well-known responses of HU treatment are the induction of HbF and increase in MCV due to the ability of the drug to induce stress erythropoiesis (6, 24, 45, 46). To assess whether MCV and/or HbF modulate differences in biophysical properties at normoxia, we categorized the patient data into low- and high-MCV and low- and high-HbF populations based on the median value for all patients. Fig. 5 shows the morphological and biomechanical properties of density-sorted red cells that have been grouped based on the median MCV value for all patients, which is about 84 fL. As shown, a statistically significant difference is observed for all properties except the cellular eccentricity ratio. Surprisingly, separation of low- and high-HbF populations according to the median HbF value for all patients did not reveal any statistically significant differences in the biophysical properties, as seen in Fig. 6.

Discussion

Although various techniques can be used for the measurement of biomechanical properties of biological cells (47), quantitative interferometric techniques are unique in that they are capable of providing 3D morphological information and biomechanical properties simultaneously for individual RBCs in a minimally invasive way. This unique feature, along with the high-throughput nature of the technique, allows for measuring hundreds of cells from sickle patients in a short period (that is, a few minutes). Although interferometric optical techniques have been used in prior studies of RBCs from sickle patients (37, 48), they were limited to the RBCs from single patients and variations of Hb concentrations in individual RBCs were not accounted for. Taking such density variations into account significantly alters the inferences derived from optical measurements because RBCs from sickle patients are known to have a wider distribution of the Hb concentrations in the cytosol than those from healthy patients (34, 35) (Fig. 2). Density fractionation of RBCs of sickle patients in this work resulted in two major improvements. First, as outlined in *Methods*, having Hb concentration for a subpopulation of RBCs allows for more precise measurements of the optically measured biophysical properties. Additionally, by measuring the cytosol viscosity using Hb density, overall changes in cell deformability can be interpreted more thoroughly.

HU treatment has been shown to reduce RBC sickling and the incidence of vasoocclusive crises in SCD patients. The mechanism through which HU brings about these benefits is, however, not well established. The antisickling benefit is believed to be mainly due to the induction of the HbF (45). Another widely known effect of the drug has been an increase in mean cell volume of RBCs (49). Strong correlation of the biophysical properties of individual RBCs with the MCV value (Fig. 5), rather than HbF (Fig. 6), suggests that the static biophysical effects of higher MCV may be the dominant drug effect at normoxia. It is, therefore, possible that the effect of HbF induction is more prominent at hypoxia, because its principal biochemical effect is to inhibit hypoxia-induced HbS polymerization. Multiple studies indeed show that, in hypoxic conditions, the effect of the HbF level correlates with the kinetic biophysical properties (29, 30, 50). These same studies do not show any drug effect for properties such as blood rheology measured at normoxic condition. The HbF content of the cells, however, is known to have more of a dominant effect on the inhibition of the sickling events. Our biomechanical and morphological measurements reveal differences between on-drug and off-drug patient populations as well as classification based on the MCV value at normoxia. One possible explanation is that static biophysical properties reported in this study reflect a combination of changes that RBCs experienced during the blood circulation. The degree and frequency of cell sickling as well as the damage to the cell membrane due to large deformations in the capillaries may all have an effect on the red cell biomechanics and morphology even at normoxia. Even the antisickling effects of HU treatment may not be rationalized by HbF induction alone (51, 52).

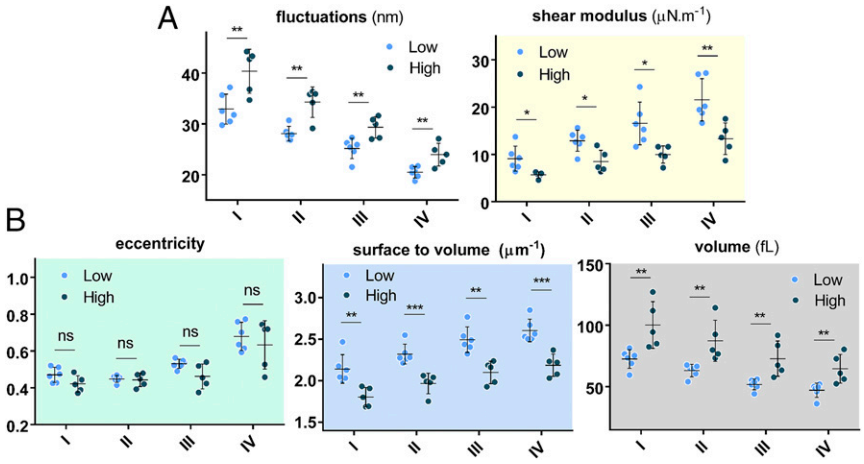

Fig. 5. Biophysical properties of RBCs of SCD patients grouped based on the MCV value of the RBCs. "Low" and "High" in these figures represent MCV values relative to the median MCV value for all patients, which is 84 fL. (*A*) Biomechanical properties as a function of the cell density and MCV value. (*B*) Morphological parameters as a function of the cell density and MCV value. Dots represent mean values for individual patients. Low MCV and high MCV are defined as the values that are less and more than the median value, respectively. The data points in each case represent the mean value, whereas the vertical error bars represent ±SD. Standard two-tailed *t* tests were used to determine the significance of the difference between two groups of data, where $*P < 0.05$, $**P < 0.01$, $***P < 0.001$, and "ns" indicates $P > 0.05$.

Therefore, our results along with recent studies suggest that the beneficial effect of HU treatment is partially through modulation of cellular biophysical properties. However, quantifying the precise contribution of these biophysical properties relative to increased HbF at the cellular level requires further development of more advanced techniques capable of measuring cellular HbF content.

Methods

Sample Preparation. Blood samples were collected under an Excess Human Material Protocol approved by the Partners Healthcare Institutional Review Board with a waiver of consent. All samples were stored at 4 °C during the shipping and storage and used within 3 d of blood harvest. Healthy whole blood was obtained from Research Blood Components. Fractionation of sickle and healthy RBCs was performed as described here in more detail (50). Briefly, OptiPrep Density Gradient Medium (Sigma-Aldrich) was used to create a stepwise gradient to separate RBCs by cell density. Using Dulbecco's PBS (HyClone DPBS; Thermo Scientific) to adjust the density of the OptiPrep medium, densities of 1.081, 1.091, 1.1, and 1.111 g/mL were made and layered in 2.5-mL volumes in order of increasing density with the densest layer on the bottom. Following two washes with PBS (HyClone; Thermo Scientific) and centrifugation at 821 × *g* at 21 °C for 5 min, cell samples were suspended in PBS to achieve a 70–80% hematocrit. Fully suspended cell suspensions were layered on the least dense layer and centrifuged at 821 × *g* for 30 min at 21 °C. Cell populations fractionated between gradient layers were isolated carefully. A population pelleted after the centrifugation was also isolated. Fractions had average densities of 1.086 ± 0.005 g/mL (density 1), 1.095 ± 0.005 g/mL (density 2), 1.105 ± 0.005 g/mL (density 3), and >1.111 g/mL (density 4). Following two washes with PBS for removal of gradient medium, fractionated cells were suspended in PBS with 1% BSA (Sigma-Aldrich) where 1 μL of pellet was suspended in 200 μL of PBS–BSA and kept at 4 °C until use.

Optical Measurements. Quantitative phase imaging (QPI) is a technique for accurately measuring the structure and function of biological samples without requiring exogenous contrast agents (53, 54). QPI is based on the principles of interferometry and measures the phase delay of the optical wave front passing through the biological samples. In simple terms, the measured phase $\Delta\phi$ is a function of RI contrast and sample height: $\Delta\phi(x,y,t) = 2\pi\Delta n h(x,y,t)/\lambda$, where $\Delta n = n_c - n_m$, and n_c and n_m are the average RIs of the cell and the culture medium, respectively. $h(x,y)$ is the cell height, and λ is the wavelength of light. In these experiments, we used $\lambda = 589$ nm and the imaging speed was 125 fps. The optical phase delay contains information on both optical properties as well as morphology of the biological samples. Diffraction phase microscope (DPM) is one such instrument that has both the common-path and off-axis features of an interferometer (31). Common-path phase microscopy entails samples and reference beams side-by-side to ensure minimal system phase noise required for measuring nanometer motions of biological samples, whereas off-axis interferometry is used to acquire single-shot interferograms beneficial for studying fast dynamics of biological systems. In the context of RBCs, these two features make DPM an excellent candidate for measuring rapid thermal fluctuations of the red cell membrane. It must be noted that RI of the Hb is related to the concentration of the Hb and could be calculated as follows: $n_c = n_w(1 + \beta c)$, where n_w is the RI of water, c is the concentration of the Hb, and β is the wavelength-dependent RI increment (55). Using the Hb concentration, the average RI has been calculated for each density category to provide a more accurate account of the red cell morphology.

Mechanical Modeling. It was first shown by Brochard and Lennon (56) that the decay rate of the thermal fluctuations of a flat lipid bilayer can be linked to the mechanical properties of the membrane. Their model was later modified to account for the geometry of the RBCs and contribution of the spectrin network beneath the lipid bilayer, the details of which can be found elsewhere (32, 38). In short, in the improved methodology, RBCs are modeled as a composite

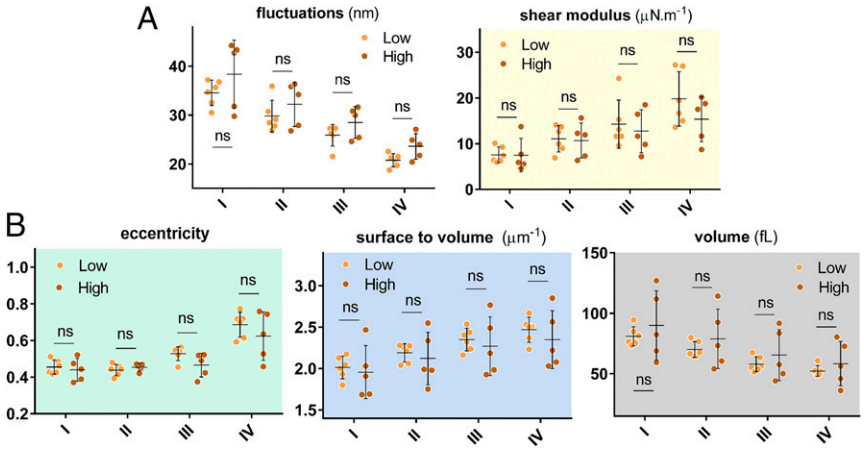

Fig. 6. Biophysical properties of RBCs of SCD patients grouped based on HbF percentage. "Low" and "High" in these figures represent HbF values relative to the median for all patients, which is 8.5%. (*A*) Biomechanical properties as a function of the cell density and HbF level. (*B*) Morphological parameters as a function of the cell density and HbF level. Dots represent mean values for individual patients. There is no statistically significant difference between patients with low and high clinically measured HbF levels. Standard two-tailed *t* tests were used to determine the significance of the difference between two groups of data, where "ns" indicates $P > 0.05$.

membrane surrounded by viscous fluids inside and outside the membrane surface. Using the experimental spatiotemporal fluctuations of the cell membrane, one can calculate the out-of-plane correlation function of the membrane at various frequencies. Thereafter, from a comparison of the theoretical prediction of the model and experimental results, one can fit for key biomechanical properties, namely, shear modulus (μ), bending stiffness (κ), and area expansion modulus (K_A) of the cell membrane, as well as the viscosity of the cytosol (η). At low frequencies, cell membrane response is dominated by the elastic properties of the cell membrane and does not vary with the chosen frequency at which mechanical parameters are calculated (32). All parameters reported in this paper have been calculated at $\omega = 10$ rad/s. Average viscosity of each subpopulation can be calculated from the relationship between microviscosity and concentration of the Hb in the cytosol (39). Micropipette measurements show the area expansion modulus of the membrane ($K_A = \mu + \lambda$) of the RBC is orders of magnitude higher than the shear modulus ($\lambda \gg \mu$). The values of cytosol viscosity (η) and area expansion modulus (K_A) therefore have been fed into the model, and bending modulus (κ) and shear modulus (μ) have been extracted from a fit between the experimental measurement of the membrane fluctuations and prediction of the analytical model.

ACKNOWLEDGMENTS. This research was supported by National Institutes of Health Grants 1R01HL121386-01A1, 9P41EB015871-26A1, 5R01NS051320, 5U01HL114476, and 4R44EB012415; National Science Foundation Grant CBET-0939511; Hamamatsu Corporation; Singapore–Massachusetts Institute of Technology Alliance for Research and Technology (SMART) Center, BioSystems and Micromechanics (BioSyM) and Infectious Diseases (ID); MIT SkolTech Initiative; and Koch Institute for Integrative Cancer Research Bridge Project Initiative.

1. GBD 2013 Mortality and Causes of Death Collaborators (2015) Global, regional, and national age-sex specific all-cause and cause-specific mortality for 240 causes of death, 1990–2013: A systematic analysis for the Global Burden of Disease Study 2013. *Lancet* 385(9963):117–171.
2. Ingram VM (1957) Gene mutations in human haemoglobin: The chemical difference between normal and sickle cell haemoglobin. *Nature* 180(4581):326–328.
3. Eaton WA, Hofrichter J (1990) Sickle cell hemoglobin polymerization. *Adv Protein Chem* 40:63–279.
4. Merkel TJ, et al. (2011) Using mechanobiological mimicry of red blood cells to extend circulation times of hydrogel microparticles. *Proc Natl Acad Sci USA* 108(2):586–591.
5. Eaton WA, Hofrichter J (1995) The biophysics of sickle cell hydroxyurea therapy. *Science* 268(5214):1142–1143.
6. Charache S, et al.; Investigators of the Multicenter Study of Hydroxyurea in Sickle Cell Anemia (1995) Effect of hydroxyurea on the frequency of painful crises in sickle cell anemia. *N Engl J Med* 332(20):1317–1322.
7. Hofrichter J, Ross PD, Eaton WA (1974) Kinetics and mechanism of deoxyhemoglobin S gelation: A new approach to understanding sickle cell disease. *Proc Natl Acad Sci USA* 71(12):4864–4868.
8. Cui S, et al. (2015) The LSD1 inhibitor RN-1 induces fetal hemoglobin synthesis and reduces disease pathology in sickle cell mice. *Blood* 126(3):386–396.
9. DeSimone J, et al. (2002) Maintenance of elevated fetal hemoglobin levels by decitabine during dose interval treatment of sickle cell anemia. *Blood* 99(11):3905–3908.
10. Goldberg MA, et al. (1990) Treatment of sickle cell anemia with hydroxyurea and erythropoietin. *N Engl J Med* 323(6):366–372.
11. Cho C-S, et al. (2010) Hydroxyurea-induced expression of glutathione peroxidase 1 in red blood cells of individuals with sickle cell anemia. *Antioxid Redox Signal* 13(1):1–11.
12. Hillery CA, Du MC, Wang WC, Scott JP (2000) Hydroxyurea therapy decreases the in vitro adhesion of sickle erythrocytes to thrombospondin and laminin. *Br J Haematol* 109(2):322–327.
13. Bartolucci P, et al. (2010) Decreased sickle red blood cell adhesion to laminin by hydroxyurea is associated with inhibition of Lu/BCAM protein phosphorylation. *Blood* 116(12):2152–2159.
14. Odièvre M-H, et al. (2008) Modulation of erythroid adhesion receptor expression by hydroxyurea in children with sickle cell disease. *Haematologica* 93(4):502–510.
15. Rodgers GP, et al. (1993) Augmentation by erythropoietin of the fetal-hemoglobin response to hydroxyurea in sickle cell disease. *N Engl J Med* 328(2):73–80.
16. Almeida CB, et al. (2012) Hydroxyurea and a cGMP-amplifying agent have immediate benefits on acute vaso-occlusive events in sickle cell disease mice. *Blood* 120(14): 2879–2888.
17. Verger E, et al. (2014) Prior exposure of endothelial cells to hydroxycarbamide alters the flow dynamics and adhesion of sickle red blood cells. *Clin Hemorheol Microcirc* 57(1):9–22.
18. Chaar V, et al. (2014) Hydroxycarbamide decreases sickle reticulocyte adhesion to resting endothelium by inhibiting endothelial Lutheran/basal cell adhesion molecule (Lu/BCAM) through phosphodiesterase 4A activation. *J Biol Chem* 289(16):11512–11521.
19. Voskaridou E, et al. (2010) The effect of prolonged administration of hydroxyurea on morbidity and mortality in adult patients with sickle cell syndromes: Results of a 17-year, single-center trial (LaSHS). *Blood* 115(12):2354–2363.
20. Lobo CL, et al. (2013) The effect of hydroxcarbamide therapy on survival of children with sickle cell disease. *Br J Haematol* 161(6):852–860.
21. Lê PQ, et al. (2015) Survival among children and adults with sickle cell disease in Belgium: Benefit from hydroxyurea treatment. *Pediatr Blood Cancer* 62(11):1956–1961.
22. Yawn BP, et al. (2014) Management of sickle cell disease: Summary of the 2014 evidence-based report by expert panel members. *JAMA* 312(10):1033–1048.
23. Steinberg MH, et al.; Investigators of the Multicenter Study of Hydroxyurea in Sickle Cell Anemia and MSH Patients' Follow-Up (2010) The risks and benefits of long-term use of hydroxyurea in sickle cell anemia: A 17.5 year follow-up. *Am J Hematol* 85(6):403–408.
24. Platt OS (2008) Hydroxyurea for the treatment of sickle cell anemia. *N Engl J Med* 358(13):1362–1369.
25. Steinberg MH, Hebbel RP (1983) Clinical diversity of sickle cell anemia: Genetic and cellular modulation of disease severity. *Am J Hematol* 14(4):405–416.
26. Schechter AN (2008) Hemoglobin research and the origins of molecular medicine. *Blood* 112(10):3927–3938.
27. Brittenham GM, Schechter AN, Noguchi CT (1985) Hemoglobin S polymerization: Primary determinant of the hemolytic and clinical severity of the sickling syndromes. *Blood* 65(1): 183–189.
28. Platt OS, et al. (1991) Pain in sickle cell disease. Rates and risk factors. *N Engl J Med* 325(1):11–16.
29. Wood DK, Soriano A, Mahadevan L, Higgins JM, Bhatia SN (2012) A biophysical indicator of vaso-occlusive risk in sickle cell disease. *Sci Transl Med* 4(123):123ra26–123ra26.
30. Higgins JM, Eddington DT, Bhatia SN, Mahadevan L (2007) Sickle cell vasoocclusion and rescue in a microfluidic device. *Proc Natl Acad Sci USA* 104(51):20496–20500.
31. Popescu G, Ikeda T, Dasari RR, Feld MS (2006) Diffraction phase microscopy for quantifying cell structure and dynamics. *Opt Lett* 31(6):775–777.
32. Park Y, et al. (2010) Measurement of red blood cell mechanics during morphological changes. *Proc Natl Acad Sci USA* 107(15):6731–6736.
33. Park Y, et al. (2008) Refractive index maps and membrane dynamics of human red blood cells parasitized by *Plasmodium falciparum*. *Proc Natl Acad Sci USA* 105(37): 13730–13735.
34. Rodgers GP, Schechter AN, Noguchi CT (1985) Cell heterogeneity in sickle cell disease: Quantitation of the erythrocyte density profile. *J Lab Clin Med* 106(1):30–37.
35. Kumar AA, et al. (2014) Density-based separation in multiphase systems provides a simple method to identify sickle cell disease. *Proc Natl Acad Sci USA* 111(41):14864–14869.
36. Hebbel RP (1991) Beyond hemoglobin polymerization: The red blood cell membrane and sickle disease pathophysiology. *Blood* 77(2):214–237.
37. Byun H, et al. (2012) Optical measurement of biomechanical properties of individual erythrocytes from a sickle cell patient. *Acta Biomater* 8(11):4130–4138.
38. Kuriabova T, Levine AJ (2008) Nanorheology of viscoelastic shells: Applications to viral capsids. *Phys Rev E Stat Nonlin Soft Matter Phys* 77(3 Pt 1):031921.
39. Gennaro AM, Luquita A, Rasia M (1996) Comparison between internal microviscosity of low-density erythrocytes and the microviscosity of hemoglobin solutions: An electron paramagnetic resonance study. *Biophys J* 71(1):389–393.
40. Evans EA (1989) Structure and deformation properties of red blood cells: Concepts and quantitative methods. *Methods Enzymol* 173:3–35.
41. Eaton JW, Jacob HS, White JG (1979) Membrane abnormalities of irreversibly sickled cells. *Semin Hematol* 16(1):52–64.
42. Clark MR, Mohandas N, Shohet SB (1980) Deformability of oxygenated irreversibly sickled cells. *J Clin Invest* 65(1):189–196.
43. Mohandas N, Gallagher PG (2008) Red cell membrane: Past, present, and future. *Blood* 112(10):3939–3948.
44. Mohandas N, Chasis JA, Shohet SB (1983) The influence of membrane skeleton on red cell deformability, membrane material properties, and shape. *Semin Hematol* 20(3):225–242.
45. Letvin NL, Linch DC, Beardsley GP, McIntyre KW, Nathan DG (1984) Augmentation of fetal-hemoglobin production in anemic monkeys by hydroxyurea. *N Engl J Med* 310(14):869–873.
46. Green NS, Barral S (2014) Emerging science of hydroxyurea therapy for pediatric sickle cell disease. *Pediatr Res* 75(1-2):196–204.
47. Bao G, Suresh S (2003) Cell and molecular mechanics of biological materials. *Nat Mater* 2(11):715–725.
48. Shaked NT, Satterwhite LL, Telen MJ, Truskey GA, Wax A (2011) Quantitative microscopy and nanoscopy of sickle red blood cells performed by wide field digital interferometry. *J Biomed Opt* 16(3):030506.
49. Queiroz AMM (2013) The mean corpuscular volume and hydroxyurea in Brazilian patients with sickle cell anemia: A surrogate marker of compliance. *J Blood Disord Transfus* 4(5):157.
50. Du E, Diez-Silva M, Kato GJ, Dao M, Suresh S (2015) Kinetics of sickle cell biorheology and implications for painful vasoocclusive crisis. *Proc Natl Acad Sci USA* 112(5): 1422–1427.
51. Fertrin KY, et al. (2014) Imaging flow cytometry documents incomplete resistance of human sickle F-cells to ex vivo hypoxia-induced sickling. *Blood* 124(4):658–660.
52. Segel GB, Simon W, Lichtman MA (2011) Should we still be focused on red cell hemoglobin F as the principal explanation for the salutary effect of hydroxyurea in sickle cell disease? *Pediatr Blood Cancer* 57(1):8–9.
53. Ferraro P, Wax A, Zalevsky Z (2011) *Coherent Light Microscopy: Imaging and Quantitative Phase Analysis* (Springer, Berlin).
54. Popescu G (2011) *Quantitative Phase Imaging of Cells and Tissues* (McGraw Hill Professional, New York).
55. Friebel M, Meinke M (2006) Model function to calculate the refractive index of native hemoglobin in the wavelength range of 250–1100 nm dependent on concentration. *Appl Opt* 45(12):2838–2842.
56. Brochard F, Lennon JF (1975) Frequency spectrum of the flicker phenomenon in erythrocytes. *J Phys* 36(11):1035–1047.

Supporting Information

Hosseini et al. 10.1073/pnas.1610435113

Table S1. Mean corpuscular volume (MCV), mean corpuscular Hb concentration (MCHC), as well as blood composition data

	Clinical measurements					
Patients	MCV, fL	MCHC, g/dL	HbS, %	HbF, %	HbA, %	HbA2, %
On-drug						
Patient I	108	36	61.4	33.0	2.9	2.6
Patient II	95	33	79.3	13.2	2.8	4.7
Patient III	84	30	89.3	4.4	1.5	4.7
Patient IV	75	37	80.7	11.7	2.5	5.1
Patient V	131	36	81.8	11.8	2.3	4.1
Off-drug						
Patient VI	97	32	84.5	4.3	6.1	5.1
Patient VII	98	36	84.7	8.2	2.4	4.8
Patient VIII	83	38	84.7	8.2	2.4	4.8
Patient IX	84	36	84.9	7.8	2.5	4.8
Patient X	83	36	84.3	8.5	2.2	5.1
Patient XI	70	36	73.0	20.6	2.9	3.5

MCV and MCHC have been obtained from complete blood count (CBC) analysis from clinical measurements. Blood composition data are extracted from gel electrophoresis experiments identifying the fraction of various Hb types in patients in this study ($n = 11$).